Fusion Engineering and Design 88 (2013) 607–610

Contents lists available at ScienceDirect

Fusion Engineering and Design

journal homepage: www.elsevier.com/locate/fusengdes

Effect of a magnetic field on stability and transitions in liquid breeder flows in a blanket

Sergey Smolentsev*, Naveen Vetcha, Mohamed Abdou

University of California, Los Angeles, CA 90095, USA

HIGHLIGHTS

- In LM blankets, coolant/breeder flows are expected to be hydrodynamically unstable.
- Possible instabilities are related to either MHD boundary layers or bulk shear layers, typically associated with high-velocity near-wall jets.
- In the mixed-convection flows, two types of turbulence, either weak or strong, have been observed.

ARTICLE INFO

Article history:
Received 7 September 2012
Received in revised form
20 December 2012
Accepted 2 April 2013
Available online 28 April 2013

Keywords:
Blanket
MHD flow
Stability and transitions
Mixed convection

ABSTRACT

We review previous studies on instabilities and transitions in magnetohydrodynamic flows in a special context of liquid-metal blanket applications. In the past, possible transitions in blanket flows were mostly attributed to instabilities in the Hartmann layers. More recent studies show, however, that the side layers can experience instabilities at sufficiently lower Reynolds numbers. This suggests that in the blanket flows, the appearance of turbulence can most likely be related to the side rather than Hartmann layers. Various factors that may affect stability in blanket flows have been discussed. In particular, buoyancy forces can result in potentially unstable inflectional velocity profiles. First computational results, illustrating possibility of instabilities and quasi-two-dimensional turbulence in vertical mixed-convection flows heated volumetrically are presented.

Published by Elsevier B.V.

1. Introduction

For decades, liquid metal (LM) breeder blankets have been designed based on simplified inertia less flow models [1]. Recent magnetohydrodynamic (MHD) studies demonstrate, however, that even in a strong reactor-type magnetic field, inertia effects are not negligible and, in fact, can be responsible for instabilities and laminar–turbulent transitions. MHD flows in rectangular ducts are of particular importance in many breeding blanket designs, where pure lithium or lead–lithium (PbLi) alloy, circulates for tritium breeding and power conversion. Such MHD flows are known to exhibit pronounced inhomogeneity compared to their hydrodynamic counterparts. In these flows, high velocity gradients can cause instabilities and eventually turbulence. In a strong blanket-type magnetic field, turbulent flows are often foreseen to be in a special form of quasi-two-dimensional (Q2D) turbulence [2]. The inhomogeneities are caused by the flow-induced electric currents that interact with the applied magnetic field resulting in a non-uniform Lorentz force, which changes the original flow in many ways. These changes, in turn, may influence the blanket performance and its efficiency by affecting the pressure losses, heat leakages into the cooling streams, tritium permeation and may even worsen the safety conditions through the flow effects on corrosion processes.

The full set of equations for liquid-metal flows in a fusion reactor blanket consists of Navier–Stokes/Maxwell equations coupled with the equations for heat and mass transport. When written in the *inductionless approximation* (the magnetic field is considered as given, without being affected by the fluid flow) the MHD equations take the following form (see, *e.g.* [3]):

$$\rho\left[\frac{\partial \mathbf{V}}{\partial t}+(\mathbf{V}\cdot\nabla)\mathbf{V}\right]=-\nabla p+\rho\nu\nabla^2\mathbf{V}+\mathbf{j}\times\mathbf{B}_0+f, \quad (1)$$

$$\mathbf{j}=\sigma(-\nabla\varphi+\mathbf{V}\times\mathbf{B}_0), \quad (2)$$

$$\nabla\cdot\mathbf{V}=0 \quad \text{and} \quad \nabla\cdot\mathbf{j}=0. \quad (3)$$

Here, $\mathbf{V}$, $\mathbf{B}_0$, $\mathbf{j}$, φ, p, and t are the fluid velocity, applied magnetic field, electric current density, electric potential, pressure, and time, whereas ρ denotes the density, ν the kinematic viscosity, and

* Corresponding author. Tel.: +1 310 7945354.
E-mail address: sergey@fusion.ucla.ed (S. Smolentsev).

0920-3796/$ – see front matter. Published by Elsevier B.V.
http://dx.doi.org/10.1016/j.fusengdes.2013.04.001

σ the electrical conductivity of the fluid. Frequently, variables are expressed in dimensionless form by using characteristic scales, such as U_0 for velocity, B_0 for magnetic field, and L as a length scale. In doing so, the balance of momentum is fully characterized by two dimensionless groups. One is the *Hartmann number* $Ha = B_0 L(\sigma/\nu\rho)^{0.5}$, the square of which represents the ratio of electromagnetic to viscous forces. The second is the hydrodynamic *Reynolds number* $Re = U_0 L/\nu$, which measures the ratio of inertial to viscous forces. The term f on the right-hand side of the momentum equation denotes a volumetric force different from the electromagnetic one, which typically represents the gravitational force. For applications in fusion with variations of the fluid density due to strong temperature gradients, $\mathbf{f}$ stands for the buoyant force (for more details, see Section 6). The contribution of buoyancy with respect to viscous forces, is described by the *Grashof number* $Gr = g\beta\Delta T L^3/\nu^2$, where β is the volumetric thermal expansion coefficient, g is acceleration of gravity, and ΔT is a characteristic temperature difference in the fluid. Typical values of these parameters are: $Ha = 10^3$–10^4, $Re = 10^3$–10^5, and $Gr = 10^7$–10^{12}. In the case of rectangular duct flows, the Hartmann length b (the half of the duct width in the direction of the applied magnetic field) is usually used as the length scale. In Section 6, Ha is constructed using dimension b, while dimension a (half of the duct size in the direction perpendicular to the applied magnetic field) is used as a length scale in the definition of Gr and Re. In the present paper, we review instabilities and transitions, which can be foreseen in conditions of either a self-cooled or a dual-coolant lead-lithium (DCLL) blanket [1]. We also present first new results for volumetrically heated MHD flows.

2. Hartmann layers

The stability of Hartmann layers, which are formed at the duct walls perpendicular to the applied magnetic field and associated transitions to turbulence have received so far the most consideration. Several theoretical studies based on the linear stability analysis in the case of ideally insulating walls have predicted a critical Re number (above which the flow in the Hartmann layer becomes unstable and eventually turbulent) to grow linearly with the Hartmann number as $Re_c = 48,000Ha$ [4], while the experimental studies predict $Re_c = 380Ha$ [5]. The linear dependence of the critical Re number on the Hartmann number is usually explained by the fact that the ratio Re_c/Ha represents the critical Re number based on the thickness of the Hartmann layer $\sim 1/Ha$ such that the instability mechanism is similar to that in ordinary boundary-layer hydrodynamics and owns its origin to the development and growth of the Tollmien–Schlichting waves. Higher critical Reynolds numbers can be expected in electrically conducting ducts due to higher dissipation losses. As a matter of fact, this type of instability and turbulence transitions are unlikely to occur in any LM blanket due to very high values of Ha such that the ratio Re/Ha is much below its critical threshold.

3. Side layers

Side (Shercliff) layers are formed at the duct walls parallel to the magnetic field and are $\sqrt{Ha}$ thicker compared to the Hartmann layers. The stability threshold for the Shercliff layers, assuming that the Hartmann layers are stable, was derived in [6] by using the linear and energy stability analysis for the case of a non-conducting duct. The two predictions for the critical Reynolds number in the limit of a strong magnetic field are $Re_c = 48,350\sqrt{Ha}$ and $Re_c = 65.32\sqrt{Ha}$ correspondingly. In this case, the ratio $Re_c/\sqrt{Ha}$ represents the critical Reynolds number based on the thickness of the Shercliff layer as the characteristic length. By comparing the two critical Reynolds numbers, one for the Hartmann and one for the side layer, it is obvious that the side layer is more unstable than the Hartmann layer. For example, if $Ha = 10,000$, the laminar–turbulent transition in the Hartmann layer can be expected at $Re_c = 3.8 \times 10^6$, while for the Shercliff layer the critical Re number is by orders of magnitude smaller: $Re_c = 6532$. This indicates that in the LM blanket flows, the appearance of turbulence can most likely be related to the instability of the side rather than Hartmann layers.

4. Ducts with electrically conducting walls

In the case of a conducting thin-wall rectangular duct, the electric current induced in the flow bulk closes its path through the Hartmann and side layers and through the adjacent walls. This electric current distribution is responsible for the formation of the so-called "M-shaped" or "M-type" velocity profile, whose distinguished features are the two symmetric high-velocity jets at the side walls along with the near-uniform core region bounded by the jets and the Hartmann layers [7]. The jets themselves are composed of two legs owing to the wall effect on one side and the gradient-free bulk flow opposed by the Lorentz force on the other side. In the wall-side leg of the jet, the velocity exhibits changes from zero at the wall to the maximum without demonstrating any special points, while in the bulk-side leg, the velocity drops from the maximum to the core value exhibiting an inflection point, where the vorticity reaches its maximum. The existence of two inflection points in the basic velocity profile suggests that under certain conditions, such a flow becomes unstable and eventually turbulent. The corresponding hydrodynamic instability is of Kelvin–Helmholtz type (also known as "inflectional instability"), which appears in the form of two rows of counter-rotating bulk vortices. Such instabilities were observed, for example, in the fully developed flows with the M-shaped velocity profile by Reed et al. [8]. The instability phenomena are however not limited to only inflectional instability. More complex, flow structures can occur due to interaction of the bulk vortices with the near-wall liquid. This kind of phenomenon is often referred to as the "vortex–wall" interaction but in the specific context of the MHD wall-bounded flows in a strong magnetic field, where the flow dynamics is essentially Q2D, this vortex–wall interaction is not yet well understood. In addition to inflectional instability, another instability mode has been recorded in the experiments [9]. In accordance with the original author's terminology [9], in the *Type I* instability, the typical flow pattern is composed of anticlockwise-rotating periodic vortices, whose center of rotation is located in the bulk-side jet leg. The source of energy supply to these vortices is the bulk-side shear layer and the primary instability mode seems to be the inflectional instability. In the *Type II* instability, the near-wall vortices are clockwise-rotating with their center of rotation in the wall-side leg of the jet. These vortices cause a breakdown of the jet structure reducing the maximum velocity and increasing its thickness compared to those in the undisturbed flow. Recently, the stability problem for a conducting rectangular duct was revisited experimentally in [10] for the large aspect ratio. The first onset of instability was observed at a critical Reynolds number mostly independent on the magnetic field strength. The measured small fluctuations remain confined to narrow regions close to the side walls, leaving the major part of the core unaffected and laminar. By increasing further the flow rate this behavior persists until a second critical Reynolds number is reached, above which perturbations amplify quickly by one or more orders of magnitude. Similar behavior (but for lower velocities and lower magnetic field strengths) has also been predicted recently in 3D numerical computations in Ref. [11], where a sudden increase in the energy of perturbations by two orders of magnitude was found as the Reynolds number increases. The linear stability analysis for this type of flows with a side-wall jet was performed in the past [12,13] and recently [14] for the Hunt flow [15], also indicating the possibility of more than one instability modes. Detailed numerical studies of vortex–wall interactions in Q2D MHD flows were recently performed in [16].

5. Factors affecting stability in blanket flows

The real blanket flows are however much more complex than the fully developed flows discussed above. Among many complicating factors, the most possible ones are: the non-uniform electrical conductivity of the walls, buoyancy forces, the presence of other two magnetic field components, spatial changes in the plasma-confining magnetic field and/or in the cross-sectional duct dimensions, changes in the flow direction and other variations in the flow conditions that make the electric current close its path not only in the cross-sectional but also in the axial planes. In addition to the fully developed flows in rectangular ducts, some developing flows have also been studied both theoretically and experimentally. Among them, MHD flows in a non-uniform magnetic field have received, perhaps, the most consideration. As examples of the experimental studies, we can refer to the classic work [17] for a slotted duct and a more recent work on the flow in a bell-type magnetic field [18] where development of the near-wall jets and associated inflectional instability were observed once the liquid metal moves through the region of a high magnetic field gradient.

6. Instabilities and transitions in buoyancy-driven flows

Here, we present first results of the ongoing computational studies of mixed convection in conditions relevant to the DCLL blanket. We consider upward flows subject to a strong transverse magnetic field perpendicular to the temperature gradient, such that the flow dynamics is Q2D. The distribution of the volumetric heat imitates heating profile $q'''(y)$ typical to blanket conditions, where q''' decays exponentially with the radial distance y, due to the slowing down of plasma neutrons: $q'''(y)=q_0\mathrm{Exp}[-(y+a)/l]$. Here, l is the decay length, and q_0 is the maximum volumetric heating at the "hot" wall $y=-a$. This distribution of the volumetric heat is responsible for buoyancy forces in the liquid, which result in asymmetric velocity profiles with a higher velocity at the "hot" wall and lower velocity at the "cold" wall $y=a$. All computations are performed for ideally insulating ducts, both electrically and thermally. These conditions correspond to MHD flows inside the insulating flow channel insert with low electrical and thermal conductivity.

First, full 3D numerical computations were performed for a vertical square duct with two radial sections as shown in Fig. 1, using the MHD code HIMAG [19]. The computations suggest that the velocity distribution does not experience significant variations along the direction of the applied magnetic field except for the thin Hartmann layers. The temperature distribution is also rather uniform in the field direction, even in the Hartmann layers. These features give a ground to use a simpler Q2D model in the form suggested in Ref. [20] for liquid-metal MHD natural-convection flows:

$$\frac{\partial U}{\partial t}+U\frac{\partial U}{\partial x}+V\frac{\partial U}{\partial y}=-\frac{1}{\rho}\frac{\partial P}{\partial x}+\nu\left(\frac{\partial^2 U}{\partial x^2}+\frac{\partial^2 U}{\partial y^2}\right)-\frac{U}{\tau}+f_x, \quad (4)$$

$$\frac{\partial V}{\partial t}+U\frac{\partial V}{\partial x}+V\frac{\partial V}{\partial y}=-\frac{1}{\rho}\frac{\partial P}{\partial y}+\nu\left(\frac{\partial^2 V}{\partial x^2}+\frac{\partial^2 V}{\partial y^2}\right)-\frac{V}{\tau}, \quad (5)$$

$$\frac{\partial U}{\partial x}+\frac{\partial V}{\partial y}=0, \quad (6)$$

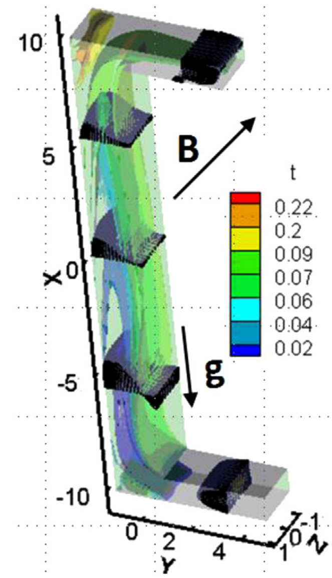

Fig. 1. 3D velocity vectors and temperature counters at $Ha=70$, $Gr=10^8$, $Re=10{,}000$.

$$\rho C_p\left(\frac{\partial T}{\partial t}+U\frac{\partial T}{\partial x}+V\frac{\partial T}{\partial y}\right)=k\left(\frac{\partial^2 T}{\partial x^2}+\frac{\partial^2 T}{\partial y^2}\right)+q'''. \quad (7)$$

In the energy equation (7), k and C_p are the thermal conductivity and specific heat. The gravity-related term $f_x=-g+g\beta(T-\bar{T})$, and $\bar{T}(x)=\frac{1}{2a}\int_{-a}^{a}T(x,y)dy$ is the mean temperature in the liquid. Parameter $\tau=bB_0^{-1}\sqrt{\rho/\sigma\nu}$ is the so-called "Hartmann braking time" [2], which is a time-scale for vortex damping due to ohmic and viscous losses in the Hartmann layers. Eqs. (4)–(7) are rewritten in the equivalent form, using the vorticity, the streamfunction and the cross-axial temperature θ ($\theta=T-\bar{T}$), and then solved numerically for a flow domain shown in Fig. 2, using periodic boundary conditions at the flow inlet/outlet. The numerical procedure is of DNS type, similar to that in Ref. [16].

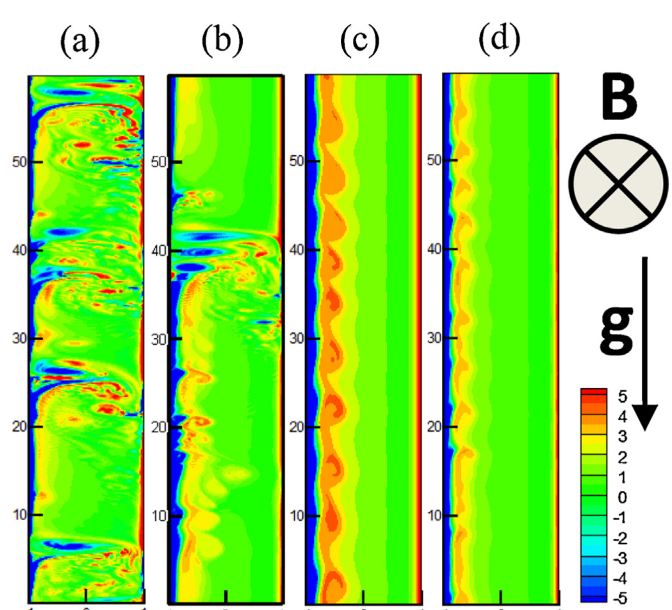

Fig. 2. Vorticity snapshots in a turbulent mixed-convection flow. Strong turbulence: (a) $Ha=50$, $Gr=10^8$, $Re=5000$; (b) $Ha=75$, $Gr=10^8$, $Re=7500$. Weak turbulence: (c) $Ha=75$, $Gr=5\times10^7$, $Re=10{,}000$; (d) $Ha=120$, $Gr=10^8$, $Re=5000$.

Effects of *Ha*, *Re* and *Gr* on turbulent flows are addressed via non-linear computations that demonstrate two characteristic turbulence regimes (Fig. 2). In the "weak" turbulence regime, the induced vortices are localized near the inflection point of the basic velocity profile, while the boundary layer at the wall parallel to the magnetic field is slightly disturbed. In the "strong" turbulence regime, the bulk vortices interact with the boundary layer causing its destabilization and formation of secondary vortices that may travel across the flow, even reaching the opposite wall. In this regime, the key phenomena are vortex–wall and various vortex–vortex interactions. Although computations are performed for relatively small Hartmann numbers, appearance of MHD turbulence in either weak or strong form seems likely to occur in the blanket flows as the Grashof numbers in the fusion blanket conditions are several orders of magnitude higher compared to those in the present computations. Higher Grashof number computations are at present not possible due to numerical limitations known in the CFD literature as "mesh Prandtl number" [21]. Further efforts are needed in the future to expand code capabilities, both 3D and Q2D, to higher *Gr* numbers.

7. Conclusions

In LM blankets, coolant/breeder flows are expected to be hydrodynamically unstable. Possible instabilities are related to either MHD boundary layers or bulk shear layers, typically associated with high-velocity near-wall jets. In the volumetrically heated mixed-convection flows, two types of turbulence, either weak or strong, have been observed, which seem to occur in the blanket conditions.

Acknowledgments

We acknowledge the support from the U.S. Department of Energy (DOE) and TITAN program under DOE Grant No. 00072621.

References

[1] S. Smolentsev, R. Moreau, L. Bühler, C. Mistrangelo, Fusion Engineering and Design 8 (2010) 1196.
[2] J. Sommeria, R. Moreau, Journal of Fluid Mechanics 118 (1982) 507.
[3] U. Müller, L. Bühler, Magneto Fluid Dynamics in Channels and Containers, Springer-Verlag, Berlin, 2001.
[4] R.J. Lingwood, T. Alboussière, Physics of Fluids 11 (1999) 2058.
[5] P. Moresco, T. Alboussière, Journal of Fluid Mechanics 504 (2004) 167.
[6] A. Pothérat, Physics of Fluids 19 (2007) 074104.
[7] J.S. Walker, Journal de Mécanique 20 (1) (1981) 79.
[8] C.B. Reed, B.F. Picologlou, Fusion Technology 15 (1989) 705.
[9] U. Burr, L. Barleon, U. Müller, A. Tsinober, Journal of Fluid Mechanics 406 (2000) 247.
[10] L. Bühler, S. Horanyi, Fusion Engineering and Design 84 (2009) 518.
[11] M. Kinet, B. Knaepen, S. Molokov, Physical Review Letters 103 (2009) 154501.
[12] K. Fajimura, UCLA-FNT-023, 1989.
[13] A.L. Ting, J.S. Walker, T.J. Moon, C.B. Reed, B.F. Picologlou, International Journal of Engineering Science 29 (1991) 939.
[14] J. Priede, S. Aleksandrova, S. Molokov, Journal of Fluid Mechanics 649 (2010) 115.
[15] J.C.R. Hunt, Journal of Fluid Mechanics 21 (1965) 577.
[16] S. Smolentsev, N. Vetcha, R. Moreau, Physics of Fluids 24 (2012) 024101.
[17] A.V. Tananaev, Flows in Ducts of MHD Devices, Atomizdat, Moscow, 1979 (in Russian).
[18] O. Andreev, Yu. Kolesnikov, A. Thess, Physics of Fluids 18 (2007) 065108.
[19] N.B. Morley, M.J. Ni, R. Munipalli, P.A. Huang, M.A. Abdou, Fusion Engineering and Design 83 (2008) 1335.
[20] T. Tagawa, G. Authié, R. Moreau, European Journal of Mechanics – B: Fluids 21 (2002) 383.
[21] J.C. Tannehill, D.A. Anderson, R.H. Pletcher, Computational Fluid Mechanics and Heat Transfer, Taylor & Francis, Washington, DC, 1997.